

SUPPORTING INFORMATION

The general fabrication process is illustrated in Figure 1.

Si wire growth. Si wires were grown from Si(111) substrate that had a low miscut angle of 0.1° . The Si was covered with 100 nm of thermal oxide. $3\mu\text{m}$ -diameter Cu particles were deposited at a $7\mu\text{m}$ pitch using photolithography. Vapor-liquid-solid (VLS) catalyzed growth of Si microwires was performed in a chemical vapor deposition (CVD) reactor with H_2 and SiCl_4 as the vapor-phase reactants [12]. For this work, the Si microwires were grown to a height of $25\mu\text{m}$ - $35\mu\text{m}$.

Surface chemical functionalization process.

Chemicals were used as received, and H_2O was obtained from a Barnstead nanopure system ($18.2\text{ M}\Omega\text{ cm}$ resistivity).

A. Cu removal

Following growth, the wire arrays were etched in buffered HF (Transene company) for 20-30 s, and then repeatedly submerged in fresh H_2O . Arrays were then heated to 65°C in a 5:1:1 solution of $\text{H}_2\text{O}:\text{HCl}:\text{H}_2\text{O}_2$ (RCA-II) for 25 min. The arrays were then rinsed with copious amounts of water, and were dried under a stream of N_2 .

B. H-termination

For hydrogen functionalization, wire arrays were submerged in buffered HF for 30 s to remove silicon dioxide. The buffered HF solution was rinsed from the arrays by repeated submersion in fresh H_2O , followed by drying under a stream of N_2 .

C. Cl-termination

Freshly etched Si wire arrays were immediately introduced to a N_2 purged glovebox that contained $< 10\text{ ppm O}_2$. Wire arrays were submerged in a saturated phosphorous(V)

chloride (PCl_5 , Alfa Aesar, 99.998% metal basis) in solution chlorobenzene (anhydrous, Sigma Aldrich, 98%) at 90 °C for 45 min. The solution was allowed to cool to near room temperature. The wire arrays were then removed from solution followed by a rinse with tetrahydrofuran THF (Anhydrous, Sigma Aldrich).

D. Methyl- and butenyl- surface functionalization

Cl-terminated Si microwire arrays were alkylated at 60 °C for > 3 h in a 0.5 M solution in THF of either CH_3MgCl (Sigma Aldrich, diluted from 3.0 M in THF) or 3-butenylMgCl (Sigma Aldrich, 0.5 M in THF). Mixed CH_3 /butenyl-terminated wire arrays were prepared by submersion of Cl-terminated wires for 10 min in 0.5 M 3-butenylMgCl in THF at 60 °C. The mixed Cl/butenyl-terminated wire arrays were rinsed with copious amounts of THF, and were then submerged in 0.5 M of CH_3MgCl for > 3 h at 60 °C.

After completion of both reactions, the Si samples were rinsed thoroughly with THF and removed from the $\text{N}_2(\text{g})$ -purged glovebox. Samples were cleaned of residual Mg salts by repeated submersion sequentially in THF, methanol, and water. Finally, the arrays were dried under a stream of $\text{N}_2(\text{g})$.

Si-PDMS matrix composite sample preparation. A 10:1 ratio mix of PDMS base and curing agent (Sylgard 184, Dow Corning) was spin-cast into a Si wire array that had been grown on Si wafer. The PDMS was then cured at 120 °C for 2 hours. The wire array was then peeled off from the substrate using a razor blade and bonded onto a clean Si wafer using a cyanoacrylate adhesive.

Carving of dog-bone shapes for tensile gripping. A Focused Ion Beam (FIB) with a Ga^+ ion source was used to mill out the T-shaped top of the wire (see Figure 1 step 6). The pull-out test was then performed by using a diamond grip.

Uniaxial Tensile Pullout Experiments. The pullout tests were performed using an in-situ nanomechanical tester, SEMentor, at a constant displacement rate of 50 nm/s. The resulting load vs. displacement data were used to calculate the interfacial shear stress by dividing by the surface area of the wires.

Calculating Interfacial Strength.

The shear lag model³⁰ was used to calculate the shear force along the sliding interface between the fiber and the matrix. Figure S1 presents a schematic that illustrates the parameters that were utilized in this derivation.

First, the shear force in the matrix was equated with the shear force at the interface using the relationships $2\pi z\tau dx = 2\pi r\tau_e dx$ and $\tau = r\tau_e/z$, where τ_e is the shear stress at the interface.

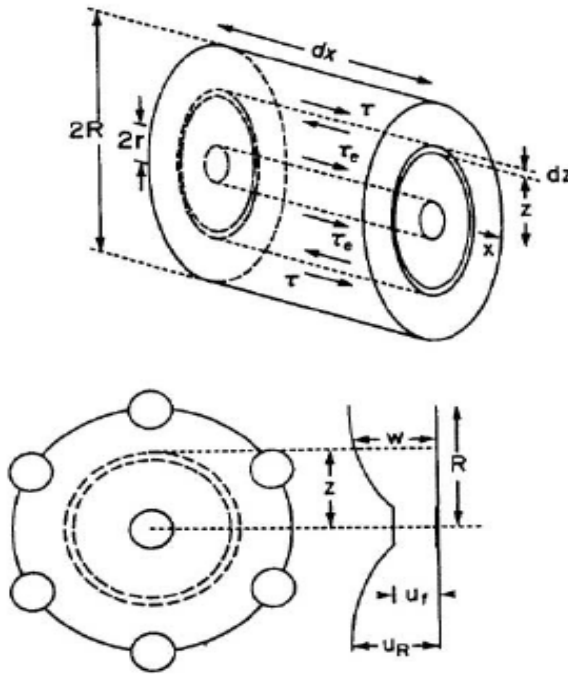


Figure S1. Schematic illustrating components of shear lag model

Ratio of shear stress τ to shear strain γ is the shear modulus, $G=E/2(1+\nu)$, giving the expression for the shear stress at the interface

$$\frac{\partial w}{\partial z} = \frac{\tau}{G_m} = \frac{\tau_e r}{G_m z}$$

Solving for the displacement at the interface, w :

$$\int_{u_f}^{u_R} dw = \frac{\tau_e r}{G_m} \int_r^R \frac{dz}{z} \text{ and } u_R - u_f = \frac{\tau_e r}{G_m} \ln\left(\frac{R}{r}\right)$$

resulting in the following expression for the equivalent shear stress:

$$\tau_e = \frac{E_m(u_R - u_f)}{2(1 + \nu_m)r \ln(R/r)}$$

The tensile force in the fiber was then equated to the shear force at the interface

$$\pi r^2 d\sigma_f = -2\pi r dx \tau_e \quad \frac{d\sigma_f}{dx} = -\frac{2\tau_e}{r} = -\frac{E_m(u_R - u_f)}{(1 + \nu_m)r^2 \ln(R/r)}$$

Differentiating and substituting for $\partial u_R / \partial x = \varepsilon_m$ and $\partial u_f / \partial x = \varepsilon_f = \sigma_f / E_f$ yields

$$\frac{d^2 \sigma_f}{dx^2} = -\frac{E_m(\varepsilon_m - \frac{\sigma_f}{E_f})}{(1 + \nu_m)r^2 \ln(R/r)}$$

This differential equation can be expressed using a dimensionless parameter, n :

$$\frac{d^2 \sigma_f}{dx^2} = \frac{n^2}{r^2} (\sigma_f - E_f \varepsilon_m) \quad n^2 = \frac{E_m}{E_f(1 + \nu_m) \ln(R/r)}$$

The solution, with A and B determined by the boundary conditions, results in:

$$\sigma_f = E_f \varepsilon_m + A \sinh\left(\frac{nx}{r}\right) + B \cosh\left(\frac{nx}{r}\right)$$

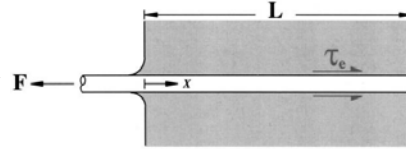
For a single fiber pullout test, the following boundary conditions are applicable: at $x=0$,

$\sigma_f = \sigma_{\max}$, and at $x=L$, $\sigma_f = 0$

The tensile strain in the matrix away from the interface is assumed to be negligible, $\varepsilon_m = 0$

This assumption gives the expression for the fiber tensile stress and shear stress at the interface

$$\sigma_f = \frac{\sigma_{\max} \sinh\left(\frac{n(L-x)}{r}\right)}{\sinh\left(\frac{nL}{r}\right)} \quad \tau_e = \frac{n\sigma_{\max} \cosh\left(\frac{n(L-x)}{r}\right)}{2\sinh\left(\frac{nL}{r}\right)}$$



The shear stress at the interface is maximized at $x=0$. De-bonding occurs when this interfacial stress exceeds a given interfacial shear stress for the system:

$$\tau_{\max} = \frac{1}{2} n \sigma_{\max} \coth(ns)$$

The resulting expression for the strain energy stored in the fiber and the matrix is:

$$\begin{aligned}
U_f &= \frac{1}{2} \int \sigma_f \epsilon_f dV = \frac{\pi r^2}{2E_f} \int_0^L \sigma_f^2 dx = \frac{\pi r^2 \sigma_{\max}^2}{2E_f \sinh^2(\frac{nL}{r})} \int_0^L \sinh^2(\frac{n(L-x)}{r}) dx = \frac{\pi r^3 \sigma_f^2}{4nE_f} \left(\coth(\frac{nL}{r}) - \frac{nL}{r \sinh^2(\frac{nL}{r})} \right) \\
U_m &= \int_0^L u_m \tau_e \pi r dx = \frac{2\pi r^2}{n^2 E_f} \int_0^L \tau_e^2 dx = \frac{\pi r^2 \sigma_{\max}^2}{2E_f \sinh^2(\frac{nL}{r})} \int_0^L \cosh^2(\frac{n(L-x)}{r}) dx = \frac{\pi r^3 \sigma_f^2}{4nE_f} \left(\coth(\frac{nL}{r}) + \frac{nL}{r \sinh^2(\frac{nL}{r})} \right) \\
U_c &= U_f + U_m = \frac{\pi r^3 \sigma_f^2}{2nE_f} \left(\coth(\frac{nL}{r}) \right) \frac{dU_c}{dL} = -\frac{\pi r^2 \sigma_f^2}{2E_f} \left(\operatorname{csch}^2(\frac{nL}{r}) \right)
\end{aligned}$$

Calculating the Work of Fracture.

Following the approach utilized by Piggott in “Load Bearing Fiber Composites,”

debonding begins when the rate of elastic energy released by the Si-PDMS composite (dU_c/dL) is equal to the rate of surface energy increase due to de-bonding (dU_s/dL) plus the rate of elastic energy stored in the debonded wire (dU_{db}/dL)

$$\frac{dU}{dL} = 0 = \frac{dU_s}{dL} + \frac{dU_{db}}{dL} + \frac{dU_c}{dL}$$

The rate of surface energy increased (dU_s/dL) is

$$\frac{dU_s}{dL} = 2\pi r G_i$$

The elastic energy stored in the de-bonded wires is (dU_{db}/dL)

$$U_{db} = \frac{1}{2} \int \sigma_f \epsilon_f dV = \frac{\pi r^2}{2E_f} \int_0^L \sigma_f^2 dx$$

Simplifying and performing the integration yields the following expression:

$$\frac{dU_{db}}{dL} = \frac{\pi r^2 \sigma_f^2}{2E_f}$$

The elastic energy of the Si-PDMS composite (U_c) is the sum of elastic energy stored in the fiber (U_f) and in the matrix (U_m)

$$U_c = U_f + U_m = \frac{\pi r^3 \sigma_f^2}{2nE_f} \left(\coth(\frac{nL}{r}) \right) \text{ with the corresponding rate of}$$

$$\frac{dU_c}{dL} = -\frac{\pi r^2 \sigma_f^2}{2E_f} \left(\operatorname{csch}^2(\frac{nL}{r}) \right)$$

Substituting the above exercised into the first equation and rearranging gives the expression for σ_f at de-bonding, and the corresponding interfacial shear stress at debonding τ_i

$$\sigma_f = \sqrt{\frac{E_f G_i}{r}} \frac{\tanh(\frac{nL}{r})}{n} \quad \text{and} \quad \tau_i = n \sqrt{\frac{E_f G_i}{r}}$$

The work of fracture from interfacial shear stress at de-bonding is then given by:

$$G_i = \frac{\tau_i^2 r}{n^2 E_f}$$

XPS acquisition and analysis

X-ray photoelectron spectroscopy (XPS) data were collected using a Kratos AXIS Ultra DLD with a magnetic immersion lens with a spherical mirror and concentric hemispherical analyzers with a delay-line detector (DLD). An Al ka (1.486 KeV) monochromatic X-ray excitation source was used. Ejected electrons were collected at an angle of 90° from horizontal. The sample chamber was maintained at $< 5 \times 10^{-9}$ Torr. High-resolution XPS data were analyzed using CasaXPS v2.3.15.

Survey scans from 0 to 1200 eV were performed to identify the elements that were present on the surface. Mg was not detected on any sample after workup. Si2p (104.5-97.5 eV) and C1s (292-282 eV) high-resolution XPS data were taken.

A simple substrate overlayer model was used here to calculate the thickness of the overlayer, d_{ov}

$$d_{ov} = \ln \left[\left(\frac{I_{ov}}{I_{Si}} \right) \left(\frac{SF_{Si}}{SF_{ov}} \right) \left(\frac{\rho_{Si}}{\rho_{ov}} \right) + 1 \right] \lambda \sin(\theta)$$

I_{ov} and I_{Si} are the signal intensity of the C_{Si} (284 eV) and Si_{bulk} 2p(3/2) XPS signals respectively. SF_{ov} and SF_{Si} are the modified sensitivity factors for the Si 2p(3/2) and C 1s signals. ρ_{ov} (0.033 mol cm⁻³ based on hydrocarbon) and ρ_{Si} (0.083 mol cm⁻³ based on Si crystal structure) are the atomic density of C in the overlayer and in the Si crystal. λ is the mean free path of electrons, determined empirically as 3.5 nm for Si 2p electrons, {haber; laibinis 1991; tufts 1992} and θ is the angle from the horizontal to the detector (90°).

Modified sensitivity factors for the specific instrument were used as determined by Kratos. In this case, $SF_{Si} = 0.174$ for the 2p(3/2) electrons and $SF_C = 0.278$.

$d_{ov} = 0.45$ for the CH₃-Si(111) surface. d_o for a methyl group is 0.468 nm, and thus gives $\theta_{CH_3-Si} = 0.96 \pm 0.05$ (based on $\Gamma_{Si(111)} = 7.83 \times 10^{14}$ cm⁻²).

Similarly, the coverage of CH₃-, mixed butenyl/CH₃-, butenyl-, and octadecyl-Si(011) were determined.

The fractional coverage of butenyl groups on the mixed butenyl/CH₃-Si(011) were estimated based on the kinetics of the 3-butenylMgCl reaction with Cl-Si(011). Figure X1.

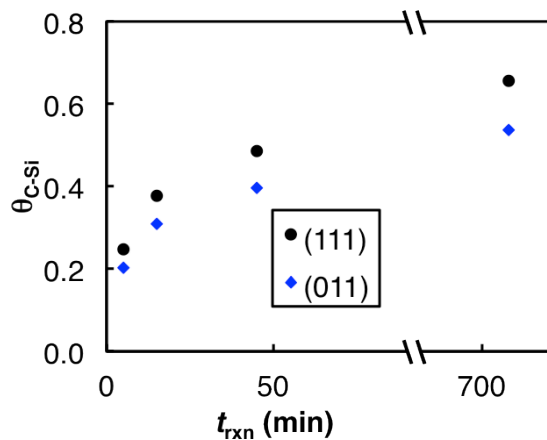


Figure S2. Coverage of butenyl groups on a Si(011) surface vs time of reaction, t_{rxn} . Coverage was based on the density of surface atoms, where $\theta_{\text{C-Si(111)}} = \Gamma_{\text{C-Si}}/\Gamma_{\text{Si(111)}}$, black dots, and $\theta_{\text{C-Si(011)}} = \Gamma_{\text{C-Si}}/\Gamma_{\text{Si(011)}}$ surface, blue diamonds.

Table X2. Summary of surface coverage.

Sample	$\theta_{\text{C-Si(011)}}$	$\theta_{\text{C-Si(111)}}$
CH ₃ -Si(111)	-	0.94 ± 0.05
CH ₃ -Si(011)	0.69 ± 0.05	0.85 ± 0.05
Mix butenyl/CH ₃	0.51 ± 0.05	0.62 ± 0.05
octadecyl	0.28 ± 0.05	0.34 ± 0.07